Pestic. Sci. 1997, **49**, 319–332

Sites of Action of Noncompetitive GABA Antagonists in Houseflies and Rats: Three-Dimensional QSAR Analysis

Miki Akamatsu,[a]* Yoshihisa Ozoe,[b] Tamio Ueno,[a] Toshio Fujita,[a] Kazuo Mochida,[b] Toshiie Nakamura[b] & Fumio Matsumura[c]

[a] Department of Agricultural Chemistry, Kyoto University, Kyoto 606-01, Japan
[b] Department of Life Science and Biotechnology, Shimane University, Matsue, Shimane 690, Japan
[c] Department of Environmental Toxicology and Department of Entomology, University of California, Davis, California 95616, USA

(Received 22 March 1996; revised version received 1 August 1996; accepted 20 November 1996)

Abstract: Quantitative structure–activity relationships for insecticidal activity (against houseflies) and competitive activity against a specific [^{35}S]*tert*-butylbicyclophosphorothionate binding (to rat brain membranes) of some picrotoxinin-type 4-aminobutyric acid antagonists, including γ-BHC, endosulfan, bicyclophosphates, dioxatricyclododecenes and related compounds, were examined three-dimensionally using comparative molecular field analysis (CoMFA). The antagonists were classified into two series according to their molecular shapes: i.e. whether their structure was 'linearly' extended beyond the 'mast-head' position of the 'boat-like' skeletons (series 1) or not (series 2). The CoMFA showed that the slopes in steric and electrostatic fields around the molecule were significant for both series in governing the potency variations in insecticidal and binding activities. Hydrophobicity, a possible factor controlling transport behaviour of compounds, was significant in governing variations in insecticidal activity, but not for the case of the rat membrane binding. Assuming that there is a slight topological difference between series 1 and 2 compounds in terms of the mode of binding with the housefly receptor site, the insecticidal activity was analysable with a single equation for the combined set of compounds, but the rat membrane binding was not. The sterically and electrostatically favourable regions surrounding the molecular series indicated by CoMFA were roughly located at positions so as to interact with the binding subsites on the receptors proposed previously.

Key words: picrotoxinin-type GABA antagonists, comparative molecular field analysis, CoMFA, insecticidal activity against houseflies, competitive activity against specific [^{35}S]TBPS binding to rat brain membranes

1 INTRODUCTION

γ-BHC and cyclodiene insecticides, such as endosulfan, mainly act as noncompetitive antagonists of 4-aminobutyric acid (GABA), an inhibitory neurotransmitter of the nervous systems of vertebrates as well as insects. It is well accepted that the site of action of these insecticides is the binding site for picrotoxinin (PTX), a classical GABA antagonist, on the $GABA_A$ receptor-chloride channel complex protein.[1–5] Structurally different types of GABA antagonists, such as 4-*tert*-butyl-2,6,7-trioxa-1-phosphabicyclo[2.2.2]octane-1-thione (*tert*-butylbicyclophosphorothionate; TBPS) and 1-(4-ethynylphenyl)-4n-propyl-2,6,7-trioxabicyclo[2.2.2]-octane (ethynylbicycloorthobenzoate; EBOB), are also believed to act at the same or an overlapping site,[6] but the structural diversity of ligands makes it difficult to understand the molecular topography of the binding mode of these toxicologically important PTX analogues.

* To whom correspondence should be addressed.

Pestic. Sci. 0031-613X/97/$17.50

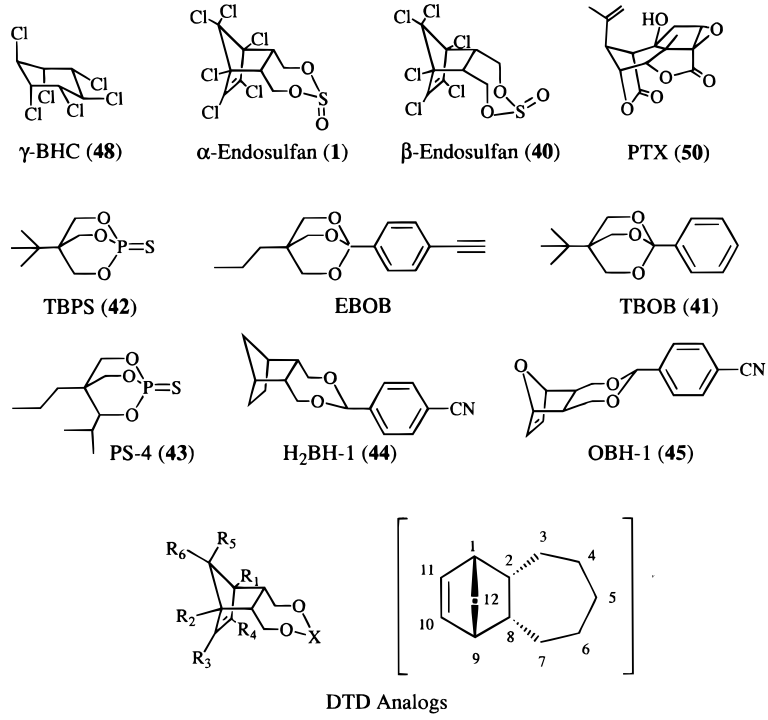

Fig. 1. Structures of compounds.

In order to study the structural requirements for the interaction of these compounds with the PTX binding site, we have synthesised a number of related compounds, as well as some 5-substituted 2,3 : 8,7-*endo*-4,6-dioxatricyclo[7.2.1.$0^{2,8}$]dodec-10-enes (DTDs) which are chlorinated at a variety of positions as shown in Fig. 1. In earlier studies, we have reported their insecticidal activity against houseflies[7,8] as well as their activity as $GABA_A$-receptor antagonists using a rat nervous system.[8] The structure–activity patterns of these GABA antagonists suggest that active ligands carry electronegative and bulky (or hydrophobic) moieties capable of interacting to various extents with subsites, A, B, C and D, in the binding region of the receptor as depicted with the structure of PTX in Fig. 2.[7–9]

In this study, to examine the previous suggestion, insecticidal activity against houseflies and competitive activity against the specific [^{35}S]TBPS binding to a rat brain membrane preparation were analysed by a three-dimensional quantitative structure–activity relationship (QSAR) procedure with use of comparative molecular field analysis (CoMFA)[10] for a set of γ-BHC, endosulfan, bicyclophosphates, dioxatricyclododecenes and related compounds. We discuss the possible topology for the receptor binding of the set of structurally diverse compounds to insect and mammalian $GABA_A$ receptors, based on the sterically and electrostatically favourable and forbidden regions on the molecule surface as indicated by CoMFA.

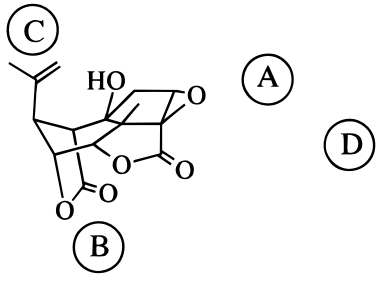

Fig. 2. Four binding subsites on the receptor.

2 EXPERIMENTAL

2.1 Chemicals

Structures of compounds are shown in Fig. 1 and Table 1. These compounds are the same as those used in earlier studies.[7,8]

2.2 Insecticidal activity

The insecticidal activity of the compounds was measured topically at 25°C against houseflies (*Musca domestica* L., a WHO insecticide-susceptible strain, three to five days old).[7,8] Log ($1/LD_{50}$) or pLD_{50} in which LD_{50} is the dose (mole per insect) required for 50% mortality was taken as the index of the topical insecticidal potency. The pLD_{50} values listed in Table 1 were adopted from our previous papers.[7,8] The pLD_{50} values for TBPS (**42**) and PTX (**50**) were not obtained topically but by injection, because of their low penetra-

TABLE 1

Insecticidal and Rat-Receptor Binding Activities, and Log *P* Values

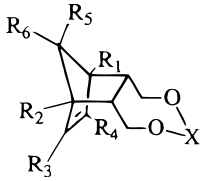

Compound									pLD_{50}					pIC_{50}			
										Calcd					Calcd		
No.	R_1	R_2	R_3	R_4	R_5	R_6	*X*	*Series*[a]	*Obsd*	*eqns (1)(2)*	Δ	*eqn (3)*	Δ	*Obsd*	*eqns (4)(5)*	Δ	*log* P[b]
1	Cl (α-Endosulfan)	Cl	Cl	Cl	Cl	Cl	S=O	2	9·99	9·75[h]	0·24	9·94	0·05	7·85	7·90[l]	−0·05	3·83[n]
2	H	H	H	H	Cl	Cl	S=O	2	<7·43	—	—	—	—	6·70	6·26[l]	0·44	2·00
3	H	H	H	H	Cl	H	S=O	2	7·64	7·88[h]	−0·24	8·16	−0·52	5·17	5·55[l]	−0·38	1·56
4	H	H	H	H	H	H	S=O	2	8·37	8·01[h]	0·36	8·30	0·07	5·80	5·81[l]	0·01	1·73
5	Cl	Cl	Cl	Cl	Cl	Cl	CH_2	2	9·53	9·30[h]	0·23	8·95	0·58	6·85	6·54[l]	0·31	3·08
6	Cl	Cl	Cl	Cl	Cl	H	CH_2	2	8·93	8·75[h]	0·18	8·69	0·24	5·92	5·83[l]	0·09	2·37
7	Cl	Cl	Cl	H	Cl	Cl	CH_2	2	8·92[c]	8·79[h]	0·13	8·55	0·37	7·36[c]	6·68[l]	0·68	2·43
8	Cl	Cl	Cl	H	H	Cl	CH_2	2	8·19[c]	8·24[h]	−0·05	8·25	−0·06	6·53[c]	6·54[l]	−0·01	1·72
9	Cl	Cl	Cl	Cl	H	H	CH_2	2	8·08	8·67[h]	−0·59	8·65	−0·57	5·60	6·00[l]	−0·40	2·26
10	H	H	H	H	Cl	Cl	CH_2	2	<7·37	—	—	—	—	5·37	5·87[l]	−0·50	1·27
11	Cl	Cl	Cl	Cl	Cl	Cl	$CH-CH_3$	2	8·42[d]	9·70[h]	−1·28	8·65	−0·23	5·43	5·53[l]	−0·10	3·60
12	Cl	Cl	Cl	Cl	H	Cl	$CH-CH_3$	2	<7·55	—	—	—	—	5·80	5·72[l]	0·08	2·89
13	Cl	Cl	Cl	H	Cl	Cl	$CH-CH_3$	2	<7·55[c]	—	—	—	—	5·74[c]	5·64[l]	0·10	2·95
14	Cl	Cl	Cl	H	H	Cl	$CH-CH_3$	2	<7·50[c]	—	—	—	—	5·46[c]	5·52[l]	−0·06	2·23
15	H	H	H	H	H	H	$CH-CH_2C_6H_5$	1	7·62	7·49[i]	0·13	7·52	0·10	<7·41	—	—	2·94
16	H	H	H	H	Cl	Cl	$CH-C_6H_4-CN-4$	1	<7·53	—	—	—	—	5·62	5·65[m]	−0·03	2·99
17	H	H	H	H	Cl	H	$CH-C_6H_4-CN-4$	1	<7·48	—	—	—	—	6·13	6·10[m]	0·03	2·56
18	H	H	H	H	H	H	$CH-C_6H_4-CN-4$	1	9·39	8·88[i]	0·51	8·57	0·82	7·04	6·78[m]	0·26	3·09[o]
19	H	H	H	H	H	H	$CH-C_6H_4-C\equiv CH-4$	1	10·61[e,f]	8·47[i]	2·14	8·42	2·19	8·49[j]	5·79[m]	2·70	3·57
20	H	H	H	H	H	H	$CH-C_6H_5$	1	8·02	8·35[i]	−0·33	8·22	−0·20	6·16	6·25[m]	−0·09	3·30
21	H	H	H	H	H	H	$CH-C_6H_4-Br-4$	1	8·14	8·67[i]	−0·53	8·74	−0·60	6·47	6·42[m]	0·05	4·16
22	H	H	H	H	H	H	$CH-C_6H_4-Cl-4$	1	8·96	8·75[i]	0·21	8·74	0·22	6·82	6·59[m]	0·23	4·01[o]
23	H	H	H	H	H	H	$CH-C_6H_4-F-4$	1	8·52	8·63[i]	−0·11	8·49	0·03	6·70	6·72[m]	−0·02	3·44
24	H	H	H	H	H	H	$CH-C_6H_4-NO_2-4$	1	8·43[e]	9·22[i]	−0·79	8·63	−0·20	5·72[j]	7·45[m]	−1·73	3·04
25	H	H	H	H	H	H	$CH-C_6H_4-Cl-3$	1	8·22	8·39[i]	−0·17	8·38	−0·16	6·77	6·54[m]	0·23	4·01
26	H	H	H	H	H	H	$CH-C_6H_4-Cl_2-3,4$	1	8·81	8·76[i]	0·05	8·84	−0·03	6·36	6·75[m]	−0·39	4·60
27	H	H	H	H	H	H	$CH-C_6H_4-Cl_2-2,4$	1	<7·49	—	—	—	—	5·51	5·45[m]	0·06	4·72
28	H	H	H	H	H	H	$CH-C_6H_4-CF_3-4$	1	<7·49	—	—	—	—	6·00	6·46[m]	−0·46	4·18
29	H	H	H	H	H	H	$CH-C_6H_4-CH_3-4$	1	<7·41	—	—	—	—	6·00	6·17[m]	−0·17	3·79

TABLE 1—*Continued*

Compound								Series[a]	pLD_{50}					pIC_{50}			log P[b]
										Calcd					Calcd		
No.	R_1	R_2	R_3	R_4	R_5	R_6	X		Obsd	eqns (1)(2)	Δ	eqn (3)	Δ	Obsd	eqns (4)(5)	Δ	
30	H	H	H	H	H	H	CH—C_6H_4—OCH_3—4	1	<7·45	—	—	—	—	5·96	5·76[m]	0·20	3·21
31	H	H	H	H	H	H	CH—Δ_3—*c*—C_6H_9	1	8·32	8·45[i]	−0·13	8·31	0·01	5·48	5·54[m]	−0·06	3·07
32	H	H	H	H	H	H	CH—*c*—C_6H_{11}	1	9·01	8·54[i]	0·47	8·58	0·43	5·77	5·54[m]	0·23	3·55
33	H	H	H	H	H	H	CH—*c*—C_8H_{15}	1	8·57	8·65[i]	−0·08	8·89	−0·32	<7·44	—	—	4·67
34	H	H	H	H	H	H	CH—*n*—C_3H_7	1	7·44	7·59[i]	−0·15	7·52	−0·08	<7·32	—	—	2·58
35	H	H	H	H	H	H	CH—*n*—C_4H_9	1	7·83	7·70[i]	0·13	7·69	0·14	6·00	6·00[m]	0·00	3·11
36	H	H	H	H	H	H	CH—*n*—C_5H_{11}	1	8·00	7·74[i]	0·26	7·84	0·16	5·82	5·81[m]	0·01	3·64
37	H	H	H	H	H	H	CH—*n*—C_6H_{13}	1	<7·40	—	—	—	—	5·43	5·45[m]	−0·02	4·17
38	H	H	H	H	H	H	CH—*n*—C_7H_{15}	1	<7·42	—	—	—	—	5·08	5·27[m]	−0·19	4·70
39	H	H	H	H	H	H	P(=O)—C_6H_5	1	8·16	8·31[i]	−0·15	8·28	−0·12	6·19	6·18[m]	0·01	2·81
40	β-Endosulfan							2	9·84	10·00[h]	−0·16	9·82	0·02	6·85	6·88[l]	−0·03	3·62[p]
41	TBOB							1	9·05	8·95[i]	0·10	8·97	0·08	7·44	7·56[m]	−0·12	2·61[o]
42	TBPS							2	9·84[g]	—	—	—	—	7·35[k]	5·24[l]	2·11	2·83
43	PS-4							2	9·87[c]	10·18[h]	−0·31	10·01	−0·14	5·51[c]	5·84[l]	−0·33	4·00
44	H_2BH-1							1	9·03	8·95[i]	0·08	8·85	0·18	7·38	7·15[m]	0·23	3·21
45	OBH-1							1	8·41	8·69[i]	−0·28	8·65	−0·24	<7·38	—	—	2·73
46	α-BHC							2	<7·46	—	—	—	—	5·25	4·82[l]	0·43	3·82[q]
47	β-BHC							2	<7·46	—	—	—	—	<7·46	—	—	3·80[q]
48	γ-BHC							2	10·10	9·88[h]	0·22	10·13	−0·03	6·52[k]	5·11[l]	1·41	3·72[q]
49	δ-BHC							2	7·67[d,f]	10·16[h]	−2·49	9·72	−2·05	5·27	5·19[l]	0·08	4·14[q]
50	Picrotoxinin (PTX)							2	9·42[g]	—	—	—	—	6·70	7·03[l]	−0·33	−1·43

[a] Compounds were classified into two series. See text for the detail.
[b] Calculated with use of the CLOGP software and modified unless noted.
[c] The asymmetry factor, log 2, was added to the original value.
[d] Excluded from the analysis of eqn (2).
[e] Excluded from the analysis of eqn (1).
[f] Excluded from the analysis of eqn (3).
[g] Obtained by injection and excluded from the analysis.
[h] Calculated by eqn (2).
[i] Calculated by eqn (1).
[j] Excluded from the analysis of eqn (4).
[k] Excluded from the analysis of eqn (5).
[l] Calculated by eqn (5).
[m] Calculated by eqn (4).
[n] From Ref. 14.
[o] Measured experimentally.
[p] From Ref. 13.
[q] From Ref. 15.

bility or low hydrophobicity, and, hence, were excluded from the analysis.

2.3 Binding activity to rat-receptor preparations

Rat brain membranes were prepared according to the method of Squires *et al.*[11] The rat brain membrane preparation was incubated with each test compound at various concentrations and [^{35}S]TBPS under prescribed experimental conditions at 25°C.[8] Log ($1/IC_{50}$) or pIC_{50}, in which IC_{50} is the concentration (M) required for 50% inhibition of the specific binding of [^{35}S]TBPS, was taken as the index of the competitive binding activity. The pIC_{50} values listed in Table 1 were adopted from our previous paper.[8] The number of compounds for which the pIC_{50} value was measurable was larger than those for which a definite pLD_{50} value was available. The PTX (**50**) value was used for the analyses in this case.

2.4 Physicochemical parameters

We used the log *P* value, where *P* is the partition coefficient in an 1-octanol/water system, as the hydrophobicity parameter of the compound. For compounds **18**, **22** and TBOB (**41**), the log *P* values were measured experimentally by a flask-shaking procedure.[12] For α- (**1**)[13] and β-endosulfan (**40**),[14] and α- (**46**), β- (**47**), γ- (**48**) and δ-BHC (**49**),[15] we used the log *P* values which were reported previously. For other compounds, the log *P* value was calculated with the use of the CLOGP system, which is a part of Medchem Software, version 3.54[16] and added 0·16, the difference between the log *P*(meas.) value (4·01) and the log *P*(calc.) value (3·85) for compound **22**.

2.5 Molecular modelling

All computations were done with the molecular modelling software package SYBYL, version 5.41.[17] To select initial conformations of compounds, we used X-ray crystallographic coordinates for reference compounds. Those for β-endosulfan (**40**), γ-BHC (**48**) and PTX (**50**) were obtained from the Cambridge Crystallographic Database.[18–20] The coordinates of α-endosulfan (**1**) were those modified from the crystal structure of β-endosulfan (**40**) for conformational switch of the cyclic sulfite moiety. The coordinates of α- (**46**), β- (**47**) and δ-BHC (**49**) were derived from those for the crystal structure of γ-BHC (**48**). The bicyclic structure of TBOB (**41**), TBPS (**42**) and PS-4 (**43**) was modelled from the crystal structure of a bicyclic phosphate $OP(OCH_2)_3CCH_3$.[21] For 5-substituted DTD derivatives, the crystal structure of 5-(3-phenoxyphenyl)-2, 3 : 8,7-*endo*-4,6-dioxatricyclo-[7.2.1.$0^{2,8}$]dodec-10-ene[22] was used with appropriate modification for the 5-substituent. The coordinates of the modified portions of these structures were calculated by use of the SYBYL standard values for bond lengths and angles. The initial coordinates thus calculated were fully optimized by the semi-empirical molecular orbital method, PM3.[23–25] For the conformation with the optimized coordinates, the atomic charges were calculated using gaussian 90 (STO-3G),[26] PM3, MNDO,[23,27,28] and CNDO/2 procedures.[29]

2.6 Superposition of compounds

We hypothesized that the fully optimized conformation of the molecules represents the biologically active form, i.e. that which serves as an antagonist. The compounds were classified into series 1 and series 2 as shown in Table 1. The active conformation of compound **18** in series 1 and that of α-endosulfan (**1**) in series 2 were selected as the reference standards on which those of other compounds in respective series were superposed. The superposition was primarily made so that the ring structures and/or the positions of endocyclic oxygen atoms are as close as possible. For DTD derivatives (compounds **2**–**39**), α- (**1**) and β-endosulfan (**40**), H_2BH-1 (**44**) and OBH-1 (**45**) belonging to series 1 as well as to series 2, the norbornene, norbornane, and oxanorbornene skeletons were placed so that the root mean square of the distances of the atomic positions from the corresponding atomic positions of the reference was as small as possible. For TBOB (**41**), TBPS (**42**), PS-4 (**43**) and α- (**46**), β- (**47**) and γ-BHC (**48**), PTX (**50**), the superposition was made so that atoms on the skeletons drawn with bold lines in Fig. 3 are located as close as possible to corresponding atoms included in ring structures of the reference compounds.

2.7 Correlation analyses by CoMFA

The analyses were done with the QSAR option of SYBYL.[10] The superposed set of active conformers were placed in a lattice of 24 × 20 × 18 (X = −10 to 14, Y = −11 to 9, Z = −9 to 9) with 2·0 Å spaces. The potential energy fields of each active conformer were calculated at lattice intersections. For the Coulombic electrostatic potential at each lattice point, the charge of + 1·0 as a probe and the atomic charges in each of the molecules were used. The steric interaction (Lennard–Jones) potential at the lattice points was calculated using the sp^3-carbon atom as a probe. The log *P* value was introduced as an additional independent variable for the hydrophobicity. The data matrix was analysed by the partial least squares (PLS) method.[30] In this procedure, the enormous number of 'original' independent lattice variables and log *P* were transformed by linear combination so that all transformed variables were orthogonal, and the standard deviation between

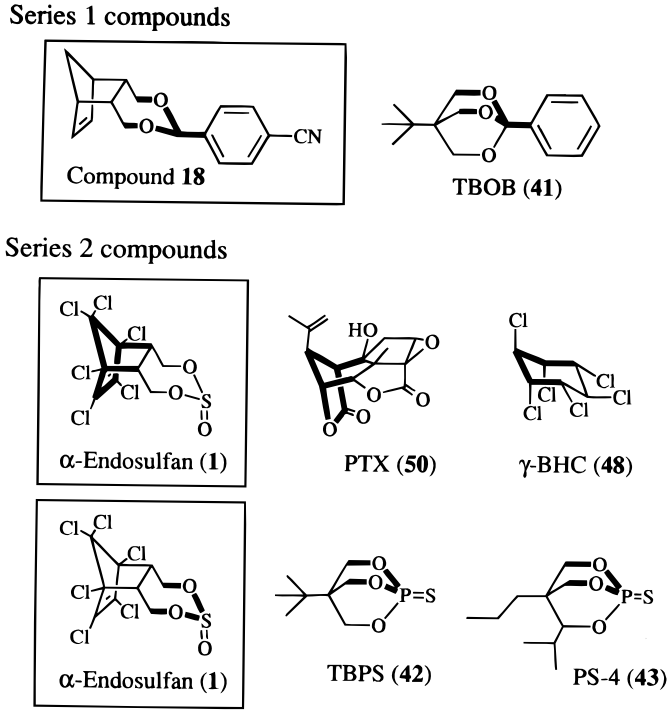

Fig. 3. Superposition procedures.

estimated and observed bioactivity indices was reduced as much as possible during the cross-validation tests. The transformed variables were usually so complex in composition that they were dealt with as latent variables. The results of the analysis were expressed as correlation equations with the number of latent variable terms used, and were displayed as contour diagrams of coefficients of the corresponding field descriptor terms at every lattice intersection to show favourable and unfavourable potential regions. We first selected the number of compounds in the set as the number of the cross-validation and then performed the analysis using the optimum number of latent variables deduced from the cross-validation tests without actual cross-validation.

Preliminary analyses were carried out for some compounds[31] in order to examine the effects of the use of various procedures to calculate atomic charges and various grid resolutions. We used the charges derived from the MNDO calculation, since the preliminary analysis was better than those with the CNDO/2, PM3 and STO-3G in gaussian 90 (equations not shown). The analyses were almost equivalent in quality, irrespective of the use of lattices with 1·0 Å, 1·5 Å and 2·0 Å spaces (equations not shown). Therefore, we selected the default value, 2·0 Å, considering the computational speed.

3 RESULTS

The pLD_{50} (houseflies) and pIC_{50} (rat brain membranes) values are listed in Table 1.[7,8] For racemic compounds **7**, **8**, **13**, **14** and PS-4 (**43**), one of two enantiomers was considered to be 'active'. Thus, the asymmetry factor, log 2, was added to the original value. Previous studies indicated that, with this treatment for racemic compounds, the predictive results from the quantitative analyses are much improved.[32,33] The pLD_{50} values are those measured under conditions such that the oxidative degradation of compounds is suppressed as far as possible (i.e. plus PBO) as the indices mimicking the potency at the insect PTX site.[7,8]

3.1 Classification of compounds

Previously, we observed that the compounds could be classified according to the effects of introduction of chlorine atoms into the norbornene moiety on the insecticidal activity and the inhibiting potency against [^{35}S]TBPS binding.[8] They are series 1 or 2 compounds depending upon the bulkiness of the 'mast-head' substituent at the 5-position in DTD derivatives and the corresponding substituents in other compounds having 'boat-like' skeletons. The introduction of four to six chlorine atoms into the norbornene moiety increased the potency of series 2 compounds with small 'mast-head' groups, whereas it decreased the potency in series 1 compounds with large 'mast-head' substituents. Series 1 compounds are likely to be capable of interacting with the D subsite of the possible receptor but series 2 compounds are not.

3.2 CoMFA for insecticidal activity

For series 1 and 2 compounds, eqns (1) and (2) were formulated, respectively, as shown in Table 2. In these and the following equations derived by CoMFA, n is the number of compounds, s and r are the conventional standard deviation and correlation coefficient, respectively. CN indicates the number of latent variables, and the cross-validated s and r are the standard deviation and the correlation coefficient from the leave-one-out cross-validation, respectively. RC refers to the relative contribution of steric and electrostatic effects, and log P to the variations in the activity.

Compounds **19** and **24** were not included in eqn (1), and compound **11** and δ-BHC (**49**) were omitted from eqn (2). The log P term was highly significant in eqn (2). It was included originally in the latent variable terms. Whereas electrostatic and steric fields are significant in eqn (1) for series 1 compounds, the hydrophobic, steric and electrostatic effects are significant in eqn (2) in rationalizing the activity variations of series 2 compounds.

Figures 4 and 5 represent the overlay of the structure of compound **18** of series 1 with the major steric and electrostatic-potential contour maps, respectively, drawn according to eqn (1). The zones covered by the

TABLE 2
Correlation Equations from CoMFA Analyses for Insecticidal Activity
$pLD_{50} = a + b \log P + [\text{CoMFA field terms}]$

							Cross-validated[b]		*RC*[c]			
Compounds	*a*	*b*	*CN*[a]	*n*	*s*	r^2	*s*	r^2	*Steric*	*Electro.*	log *P*	*eqn no.*
Series 1	8·138	—	2	18[d]	0·285	0·757	0·401	0·519	0·531	0·469	—	(1)
Series 2	6·986	0·763	1	11[e]	0·308	0·888	0·419	0·794	0·054	0·234	0·712	(2)
Series 1, 2	8·270	0·370	4	31[f]	0·332	0·814	0·559	0·475	0·370	0·517	0·113	(3)

[a] Number of components.
[b] Obtained from the leave-one-out cross-validation.
[c] Relative contribution.
[d] Compounds **19** and **24** were excluded from the analysis.
[e] Compound **11** and δ-BHC (**49**) were excluded from the analysis.
[f] Compound **19** and δ-BHC (**49**) were excluded from the analysis.

contour nets of 'shaded' broken lines in Fig. 4 and the following steric contour maps indicate regions where the submolecular bulk is well accommodated with increase in the activity, whereas the unbroken network zones are regions where the submolecular bulk is unfavourable leading to decrease in the activity. The zones covered by the nets of 'shaded' unbroken lines in Fig. 5 and the following electrostatic field maps indicate regions where the more negative electrostatic interaction with the receptor binding site increases the activity, whereas those covered by broken lines show regions where the reverse is the case.

Figure 4 indicates that steric bulk of the molecular set in the region around the 3′- and 4′-substituents on the benzene ring at the 5-position of the dioxatricycloalkene is favourable toward activity. The region occupied by these substituents could fit the D subsite in Fig. 1. It also shows that a greater steric bulk in the zone above the benzene ring, which corresponds to the location of the phenyl moiety in the benzyl group of compound **15**, reduces activity. Figure 5 shows that electron-withdrawing substituents at the 4′ position are favourable toward activity. A negative electrostatic-potential region on the molecule favourable to activity appears

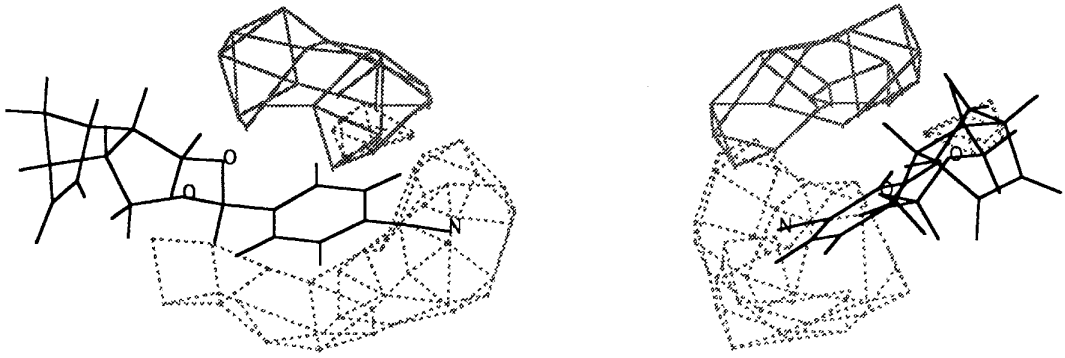

Fig. 4. Orthogonal views of the steric field map for series 1 compounds according to eqn (1) with compound **18** inserted. The contours (shaded lines) surround regions where a higher steric bulk increases (broken lines) or decreases (solid lines) the insecticidal activity at the 0·01 coefficient level.

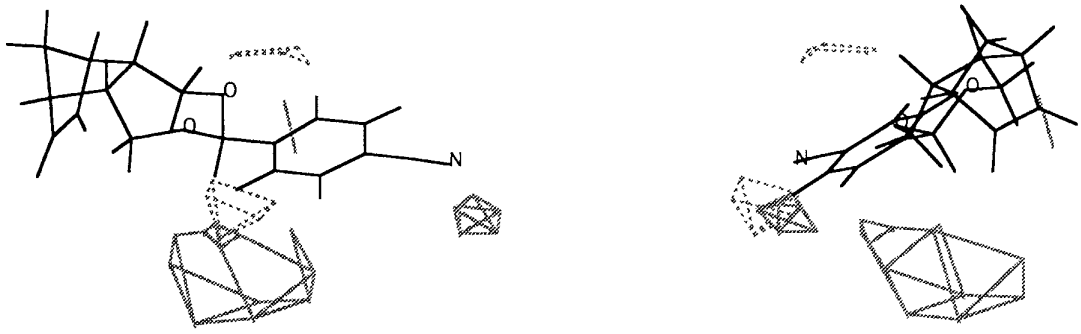

Fig. 5. Orthogonal views of the electrostatic field map for series 1 compounds according to eqn (1) with compound **18** inserted. The contours (shaded lines) surround regions where a negative (solid lines) or positive (broken lines) electrostatic potential increases the insecticidal activity at the 0·01 coefficient level.

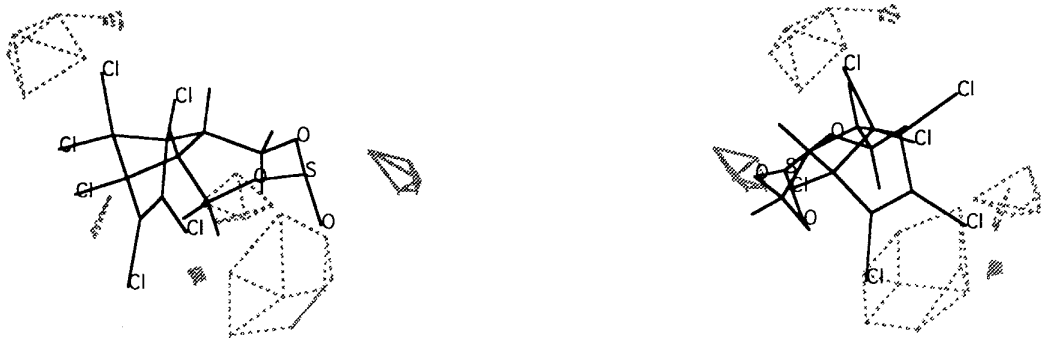

Fig. 6. Orthogonal views of the steric field map for series 2 compounds according to eqn (2) with α-endosulfan (**1**) inserted. The contours (shaded lines) surround regions where a higher steric bulk increases (broken lines) or decreases (solid lines) the insecticidal activity at the 0·002 coefficient level.

below the dioxatricycloalkene skeleton so as to accommodate two oxygen atoms. This region is likely to interact with the A binding subsite in Fig. 2 which could be electropositive. Because the R_1–R_6 groups of the active compounds used for the analysis are fixed to hydrogen atoms for most series 1 compounds, no significant contour appears in the region surrounding the cyclopenteno-moiety of the norbornene skeleton and the existence of the B and C subsites is not suggested distinctly.

Figures 6 and 7 are steric and electrostatic contour maps, respectively, for series 2 compounds with α-endosulfan (**1**). Figure 6 shows that regions around the R_5 group and the 'endo'-side of the R_3 and R_4 groups are sterically permissible, being likely to interact with the C and B subsites, respectively. Figure 6 also indicates a sterically forbidden region 'in front of' the 5-position of the DTD analogues such as the region facing to the —O—S(=O)—O— moiety of α-endosulfan. Figure 7 shows a negative electrostatic-potential region surrounding the 4-, 5- and 6-positions of DTDs which could interact with the A subsite in Fig. 2. In series 2 compounds such as α- (**1**) and β-endosulfan (**40**), γ-BHC (**48**) and 5-unsubstituted hexachloro DTD (**5**), the bulkiness of substructures is low and the electronegative character is distributed close to the region corresponding to the 5-position of the DTD analogues. As a result, they show high insecticidal activity. The R_5 group of these compounds is a chlorine atom which fits into the sterically permissible C binding subsite. The activity increases with steric bulk and an electropositive potential in the region below the two oxygen atoms in the ring, conforming to the high insecticidal activity of TBPS (**42**) and PS-4 (**43**).

Series 1 and 2 compounds could be bound to a common critical site with similar orientations, but the bulkiness and the conformation of chlorine atoms on the norbornene ring appear to be decisive as regards their binding capability.[8] We explored whether the combined set of series 1 and 2 compounds can be analysed together by CoMFA.

First, the ring structure of series 2 compounds was superposed directly on that of series 1 compounds, so that the skeletons of the DTD derivatives belonging to the two series are as close as possible. Since the phenyl group at the 5-position of dioxatricycloalkenes in series 1 compounds is projected into the sterically unfavourable region (contour map not shown), the high potency of some series 1 compounds was not well predicted. We next modified the relative orientation of the norbornene ring between series 1 and 2 compound sets, so that the sterically unfavourable region in Fig. 6 for series 2 compounds is accommodated in the sterically unfavourable region above the 5-phenyl group for series 1 compounds in Fig. 4. The modification was made by rotating the superposed set of series 1 compounds relative to the

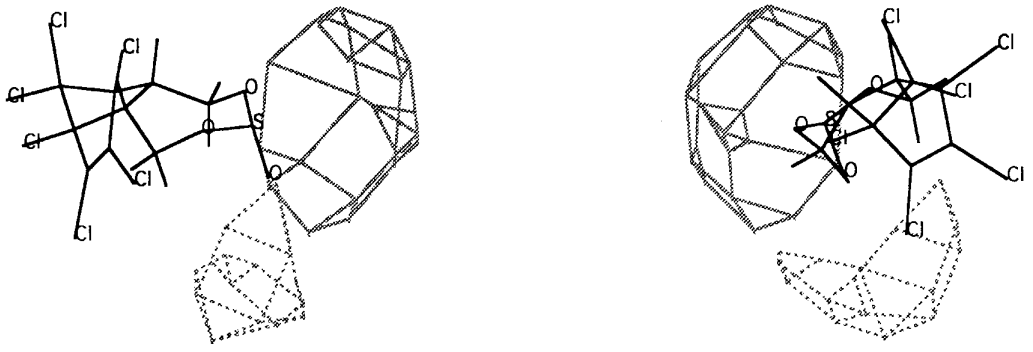

Fig. 7. Orthogonal views of the electrostatic field map for series 2 compounds according to eqn (2) with α-endosulfan (**1**) inserted. The contours (shaded lines) surround regions where a negative (solid lines) or positive (broken lines) electrostatic potential increases the insecticidal activity at the 0·005 coefficient level.

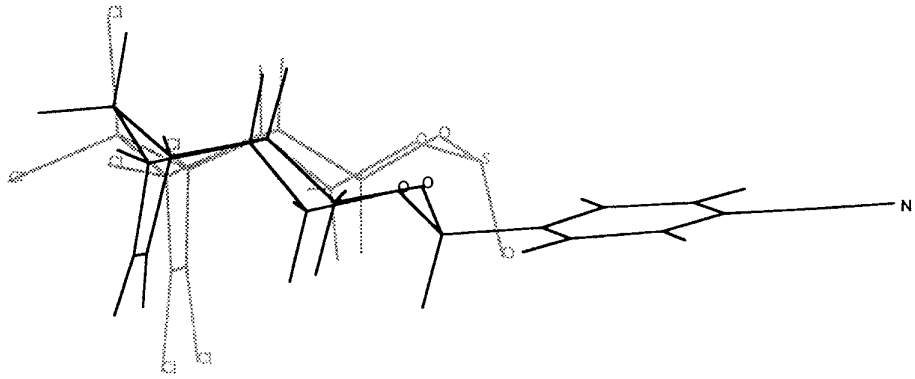

Fig. 8. Superposition of series 1 and 2 compounds. Series 2: α-endosulfan (**1**, shaded line) and series 1: compound **18** (solid line).

series 2 compound set approximately 15° clockwise with the C_2-C_8 bond in the DTD structure as the common axis. The superposition of compound **18** of series 1 and α-endosulfan (**1**) of series 2 is drawn in Fig. 8.

The CoMFA for the pLD_{50} value of the combined series 1 and 2 compounds was examined with this 'superposition' from which eqn (3) was formulated in Table 2. Although the quality of eqn (3) is lower than those of eqns (1) and (2) in terms of the cross-validated *s* and *r* (Table 2), it seems still acceptable. The result indicates that the ligands of the two series are bound to an almost identical receptor site through interactions with ligand substructures not necessarily identical between the two series. In eqn (3), only compound **19** (series 1) and δ-BHC (**49**, series 2) are not included, but compounds **11** (series 2) and **24** (series 1) are accommodated.

Since the activity of compound **19** in series 1 was much higher than expected from eqns (1) and (3), it was excluded from the analyses. Compound **18** was included in eqns (1) and (3), but the measured pLD_{50} values was also higher than the calculated value as shown in Table 1. It is likely that a narrow stick-like electronegative 4′-substituent such as cyano (**18**) or ethynyl (**19**) on the benzene ring of dioxatricycloalkenes has an additional effect on their insecticidal activity.

δ-BHC (**49**) showed a potency about three orders lower than that of γ-BHC (**48**), which was one of the most active compounds. Earlier studies showed that γ-BHC was a strong convulsant in mammals, whereas α-BHC and δ-BHC acted as anticonvulsants or depressants,[34] which could be due to positive modulatory effects at GABAergic synapses.[35] Thus, δ-BHC (**49**) was excluded from eqns (2) and (3).

The correlation results were not improved by any other alignments to combine the series 1 and 2 compound sets. With the decrease in the number of outliers, the classification of series 1 and 2 compounds and their topological modification at the binding subsite are well rationalized by the CoMFA model in terms of eqn (3). The pLD_{50} values calculated by eqn (3) are also listed in Table 1. Figures 9 and 10 are steric and electrostatic field maps, respectively. In these figures, features of molecular fields for two individual series seem to be well combined. In Fig. 9 the sterically prohibited region appears above the benzene ring at the 5-position and extends to cover the dioxaheptane ring of DTD analogues and the corresponding cyclic sulfite moiety of α-endosulfan. A sterically favourable region is shown around the R_2 and R_3 groups. Figure 10 displays a large electronegative region accommodating the 5-substituted phenyl groups of DTD analogs which may interact with the A binding subsite.

3.3 CoMFA for rat-receptor binding activity

Equations (4) and (5) were formulated for the pIC_{50} value of series 1 and 2 compounds, respectively, as shown in Table 3. Compounds **19** and **24** were excluded from eqn (4) as well as from eqn (1), and TBPS (**42**) and γ-BHC (**48**) were not included in eqn (5). The log *P* term was insignificant in eqns (4) and (5) for the binding

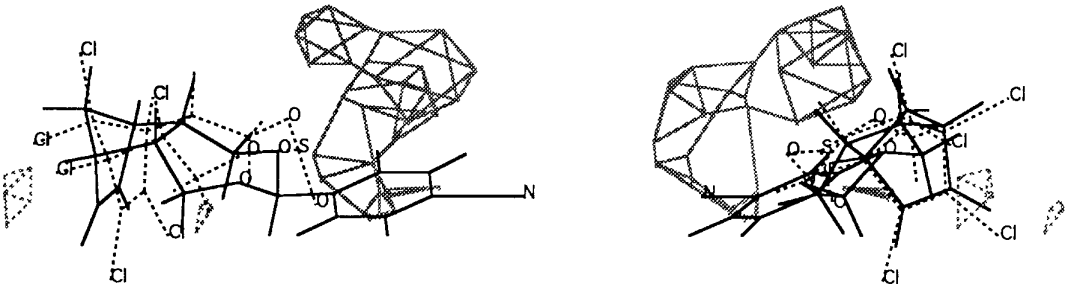

Fig. 9. Orthogonal views of the steric field map for the combined set of compounds according to eqn (3) with α-endosulfan (**1**) (broken lines) and compound **18** (solid lines) inserted. The contours (shaded lines) surround regions where a higher steric bulk increases (broken lines) or decreases (solid lines) the insecticidal activity at the 0·03 coefficient level.

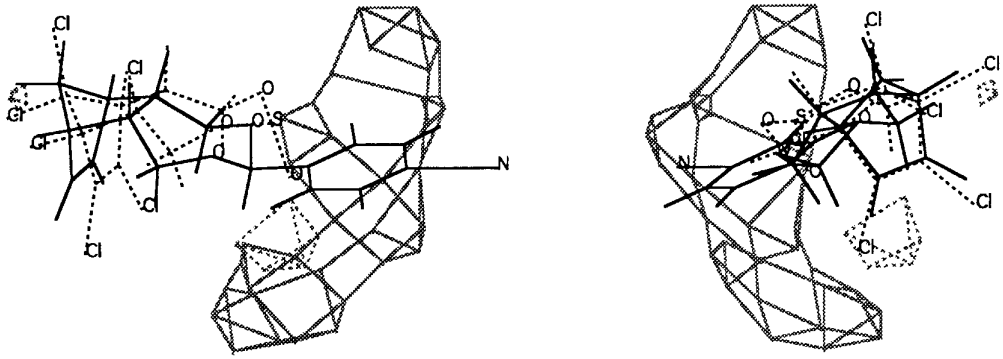

Fig. 10. Orthogonal views of the electrostatic field map for the combined set of compounds according to eqn (3) with α-endosulfan (**1**) (broken lines) and compound **18** (solid lines) inserted. The contours (shaded lines) surround regions where a negative (solid lines) or positive (broken lines) electrostatic potential increases the insecticidal activity at the 0·02 coefficient level.

activity. The pIC_{50} values calculated by eqns (4) and (5) are shown in Table 1. No significant correlation for the binding activity of the combined set was obtained with the same topological adjustment as that made for the analysis of insecticidal activity.

Figures 11 and 12 show compound **18** with the steric and electrostatic contour maps, respectively, drawn for series 1 compounds according to eqn (4). Figure 11 indicates the sterically unfavourable regions not only above but also below the benzene ring at the 5-position of dioxatricycloalkenes as well as a region outside the 4′-position of the benzene ring. The normal alkyl chain end in compounds **37** and **38** as well as the edge of the cyclohexenyl group in compound **31** reaches the sterically unfavourable region to reduce the activity. Figure 12 shows that the regions close to the 4′-substituent and below the —O—CH—O— moiety are those where the electronegative potential is favourable.

Figures 13 and 14 are steric and electrostatic contour maps, respectively, for series 2 compounds with α-endosulfan (**1**) according to eqn (5). Figure 13 shows that the sterically favourable regions of the molecular set covering the R_3 and R_4 substituents fit into the B binding subsite, and those outside the R_5 and R_6 substituents into the C subsite. Figure 13 also indicates a sterically prohibited space surrounding the

TABLE 3

Correlation Equations from CoMFA Analysis for Activity for Inhibiting Specific [^{35}S]TBPS Binding (Rat-Receptor Binding Activity)

$pIC_{50} = a + [\text{CoMFA field terms}]$

						Cross-validated[b]		*RC*[c]		
Compounds	*a*	*CN*[a]	*n*	*s*	r^2	*s*	r^2	*Steric*	*Electro.*	*eqn no.*
Series 1	6·615	4	22[d]	0·214	0·907	0·499	0·496	0·452	0·548	(4)
Series 2	4·701	4	19[e]	0·355	0·843	0·712	0·370	0·423	0·577	(5)

[a] Number of components.
[b] Obtained from the leave-one-out cross-validation.
[c] Relative contribution.
[d] Compounds **19** and **24** were excluded from the equation.
[e] TBPS (**42**) and γ-BHC (**48**) were excluded from the equation.

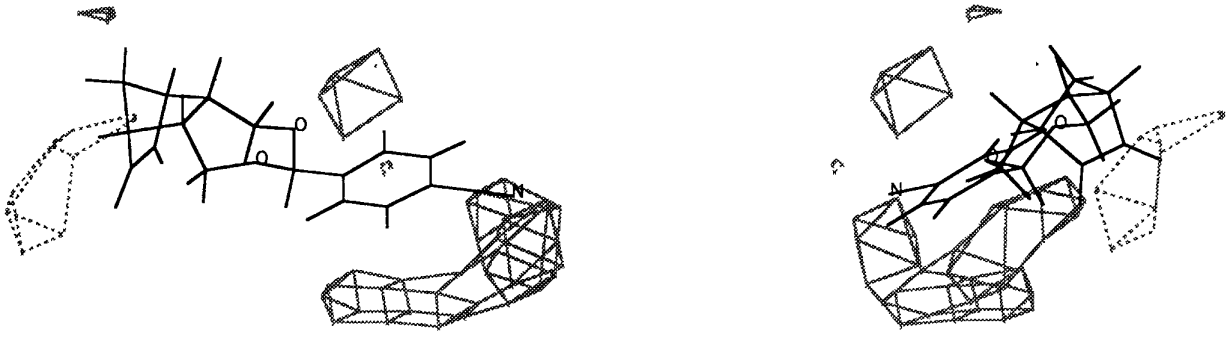

Fig. 11. Orthogonal views of the steric field map for series 1 compounds according to eqn (4) with compound **18** inserted. The contours (shaded lines) surround regions where a higher steric bulk increases (broken lines) or decreases (solid lines) the binding activity to rat brain membranes at the 0·02 coefficient level.

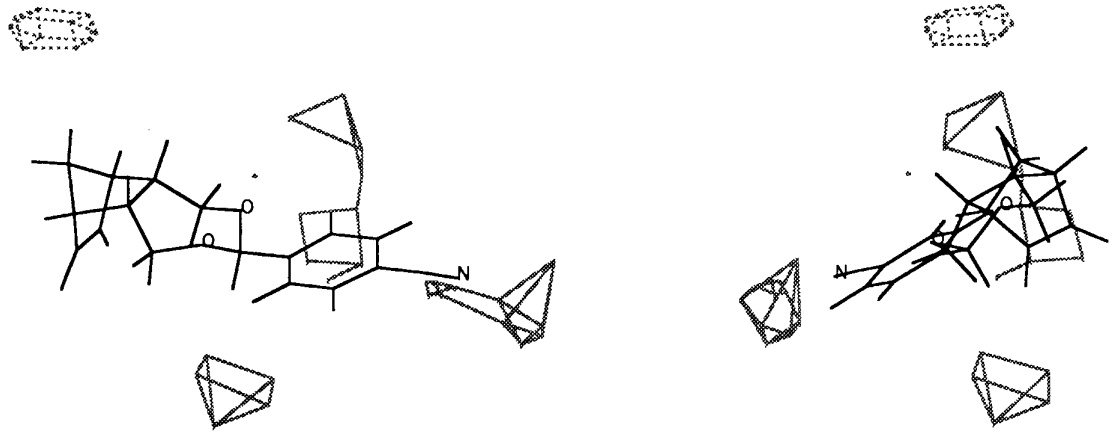

Fig. 12. Orthogonal views of the electrostatic field map for series 1 compounds according to eqn (4) with compound **18** inserted. The contours (shaded lines) surround regions where a negative (solid lines) or positive (broken lines) electrostatic potential increases the binding activity to rat brain membranes at the 0·02 coefficient level.

—O—S(=O)—O— moiety of α-endosulfan. In Fig. 14, the electropositive field favourable to the activity emerges at a region close to the R_5 position of α-endosulfan. This region could interact with the C binding subsite. Because the sign of the electrostatic potential is the reverse of that previously assumed, the electrostatic nature of the C binding subsite could be negative. Figure 14 suggests that the electronegative potential on the R_3 and R_4 positions is favourable for the interaction with the B binding subsite. The electronegative potential on the —S(=O)— moiety of α-endosulfan (**1**) works to increase its binding activity. Figure 14 also indicates that the greater the negative electrostatic potential in the region corresponding to the two oxygens in the ring, the more unfavourable it is to the activity.

The reason why TBPS (**42**) was predicted to be exceptionally inactive by eqn (5) is unclear. We have been

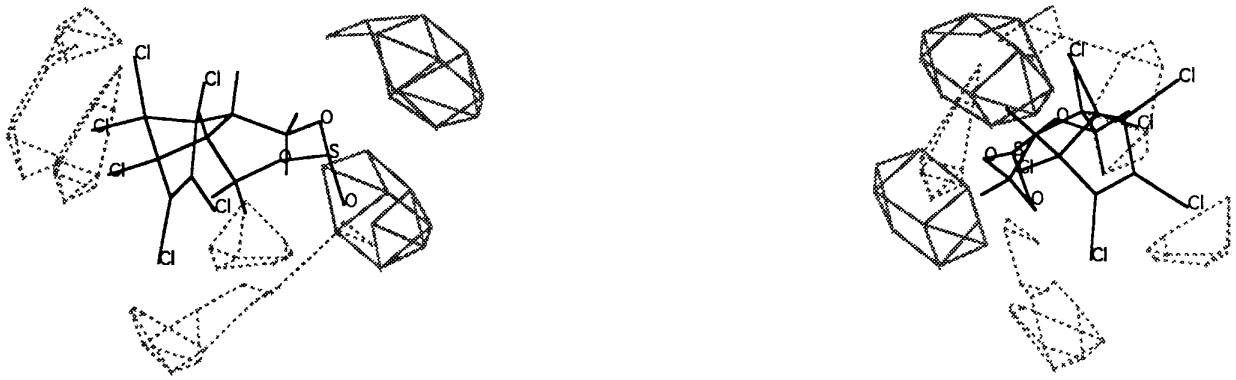

Fig. 13. Orthogonal views of the steric field map for series 2 compounds according to eqn (5) with α-endosulfan (**1**) inserted. The contours (shaded lines) surround regions where a higher steric bulk increases (broken lines) or decreases (solid lines) the binding activity to rat brain membranes at the 0·03 coefficient level.

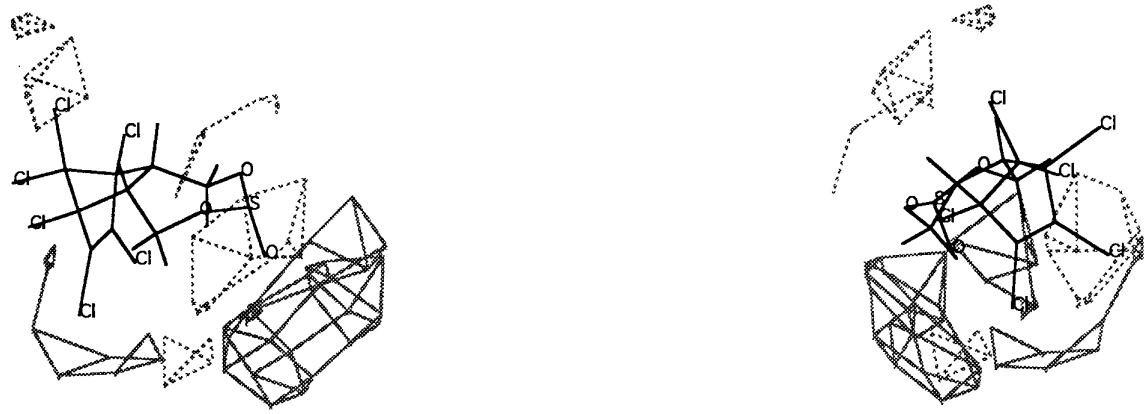

Fig. 14. Orthogonal views of the electrostatic field map for series 2 compounds according to eqn (5) with α-endosulfan (**1**) inserted. The contours (shaded lines) surround regions where a negative (solid lines) or positive (broken lines) electrostatic potential increases the binding activity to rat brain membranes at the 0·03 coefficient level.

observing the inhibition of the specific [^{35}S]TBPS binding, but this system may give a specific effect on TBPS itself. γ-BHC was also excluded from eqn (5), but α- (**46**) and δ-BHC (**47**) were accommodated in the equation despite the fact the latter two are rather anticonvulsive.[34]

4 DISCUSSION

The CoMFA contour maps shown above for series 1 and 2 GABA antagonists were combined and/or schematized so that sterically and electrostatically permissible or forbidden regions on the molecules could be recognized in a more straightforward manner in comparison with subsites A, B, C and D proposed above to exist in the binding region of the receptor (Fig. 2). In Figs 15 and 16, the schematized molecular fields are drawn for insecticidal activity and rat-receptor binding, respectively, with the 5-phenyl DTD skeleton inserted. Because some compounds which are not included in analysing the pLD_{50} value are included in analysing the pIC_{50} value, comparison between Figs 15 and 16 should not be made in too much detail. Nevertheless, similarities and dissimilarities recognizable between Figs 15 and 16 may be useful in rationalizing analogies and differences in structure–activity patterns of insecticidal and rat-receptor binding activities.

Figures 15 and 16 suggest that more than four subsites could exist in the binding domain on housefly and rat receptors, including those supposed to be the A, B, C and D subsites. The A binding subsite appears to be defined largely as having affinity for the corresponding electronegative region on the ligand molecular set in rats as well as in houseflies. This electronegative molecular region appears to be spread so as to cover the 5-

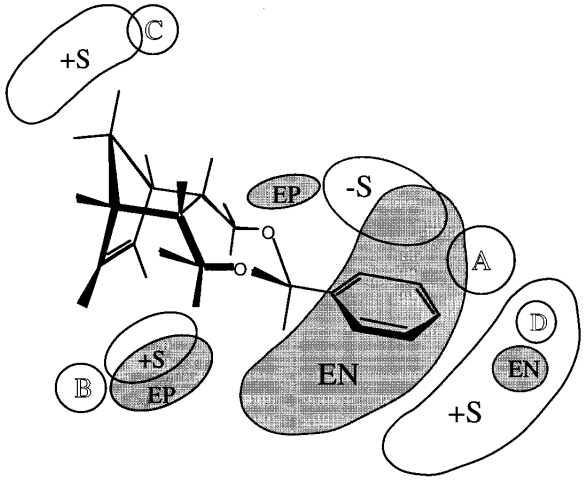

Fig. 15. Simplified steric and electrostatic molecular fields around the molecule favourable to insecticidal activity of GABA antagonists. + S and − S denote sterically permissible and forbidden regions, respectively. EN and EP are the electronegative and electropositive potential regions, respectively. The four major binding subsites on the receptor are shown with the outline font.

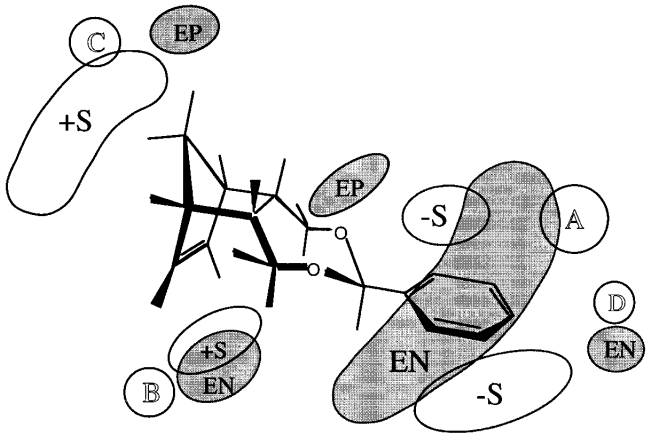

Fig. 16. Simplified steric and electrostatic molecular fields around the molecule favourable to rat-receptor binding of GABA antagonists. The notations are the same as those in Fig. 15. The four major binding subsites on the receptor are shown with the outline font.

phenyl substituent of DTD derivatives. Beyond the 4′-position of the 5-phenyl group, another region with the electronegative character is assumed to exist interacting with the D subsite on both houseflies and rat brain membrane receptors, although this region overlaps the sterically favourable region in houseflies. Subsites B and C with which corresponding steric bulk on the ligands interacts favourably are shown below and above the cyclopenteno-moiety in each figure.

One of the conspicuous differences between Figs 15 and 16 is that the ligand electropositive potential region confronts the B subsite in houseflies, whereas a more electronegative region is favoured for the interaction of this subsite in rat membranes. This is reflected in the contrast between the high insecticidal activity and low rat-receptor binding potency of PS-4 (**43**). The partially positively charged isopropyl group at the 3-position of this compound is accommodated within the sterically permissible and electronegative receptor B subsite in houseflies but not within the apparently more electropositive B subsite in rat brain membrane. Another difference is the existence of the sterically prohibited region below the benzene ring at the 5-position of DTD analogues for rat receptors. This region may partly rationalize the different structure–activity pattern between housefly and rat receptors for compounds **34**–**38** with C_3–C_7 alkyl groups at the 5-position. The rat-receptor binding activity decreases as the alkyl chain length grows, whereas the C_5-analogue shows the highest insecticidal activity. This could be due to the fact that the space available for the 5-alkyl chain for the insecticidal activity is more widely opened than that for the rat-receptor binding.

We have shown previously that there is a rough linear correlation between pLD_{50} and pIC_{50} values ($r = 0{\cdot}81$) for the present series of GABA antagonists of which both bioactivity indices were measurable ($n = 29$).[8] Considering that the correlation has been

made without classification of antagonists and that there are also dissimilarities in structure–activity patterns between insecticidal and rat-receptor binding activities, the present results summarized as Figs 15 and 16 can be taken as being reasonable.

Palmer and Casida[36] have also reported that noncompetitive GABA antagonists appear to fall into two groups based on correlations between their inhibitory potency against the [^{35}S]TBPS binding to mouse brain membrane preparations and their toxicity to mice. Whereas polychlorocycloalkanes, PTX and 2,6,7-trioxabicyclo[2.2.2]octanes which possess large 1-substituents exhibited a high potency in the in-vitro brain membrane preparation relative to their toxicity, trioxabicyclooctanes which possessed small 1-substituents and tetramethylenedisulfotetramine showed a much lower in-vitro potency than that expected from their toxicity. In this study, the compounds were differentiated into two series because of observations similar to those reported by Palmer and Casida.[36]

For the analyses of insecticidal activity against houseflies, a topological difference was considered for the mode of interaction with receptor sites between two series of GABA antagonists. The analysis was possible with the combined set of compounds. For the competitive binding activity to the rat preparation, reasonable analyses were obtained only separately for individual series of compounds. We have previously shown that the mode of binding of series 1 (**18**) and 2 (**5**) compounds to the rat-brain receptor preparation are competitive with each other, based on the use of the Scatchard analyses. Our results, and observations by others,[36,37] suggest that the mode of binding of GABA antagonists should be considered carefully with the differentiation into subgroups according to structural features.

Recently, Calder *et al.*[38] have reported a CoMFA analysis of a set of GABA antagonists which does not include DTD derivatives but otherwise is similar to that used in this study. From the analyses of in-vivo (toxicity to houseflies) and in-vitro data (the inhibition of a specific binding of [^{3}H]EBOB to housefly head membranes), they have pointed out that there is a certain similarity in CoMFA fields for GABA antagonists to interact with the receptor sites between in-vivo and in-vitro housefly activities. The present study used different animal preparations between in-vivo toxicity and in-vitro binding data. Thus, examinations of the competitive binding assay of compounds including DTD derivatives with the use of housefly preparations are apparently needed to compare with their results.

In a recent paper using housefly-head membranes, Cole *et al.*[39] have observed that polychlorocyclic insecticides such as α- (**1**) and β-endosulfan (**40**), and γ-BHC (**48**) compete directly for the [^{3}H]α-endosulfan site, whereas other channel blockers such as EBOB bind with different kinetics or at a different site. Much remains to be clarified in terms of the mode of action of GABA antagonists with the use of competitive binding assay as well as the present type of QSAR analysis. In CoMFA, one of the critical procedural steps is the strategy for constructing the superposed set of compounds. The superposition procedures of caged compounds with DTD derivatives, shown in Fig. 3, should also be further examined in terms of whether the QSAR quality is improved by topological modifications.

Recently, a cyclodiene-resistant gene was cloned from a mutant of *Drosophila melanogaster* Meig. resistant to cyclodienes and PTX.[40] Resistance was correlated with the single amino acid replacement Ala^{302} > Ser, and cyclodiene insecticides and PTX were suggested to interact with a site near Ala^{302}. In addition to structure–activity studies, such biochemical approaches may give invaluable clues as to the role of the substructures of ligands in the interaction with the PTX binding site.

ACKNOWLEDGEMENTS

We thank Drs Masumi Yamakawa and Kiyoshi Ezumi of Shionogi Research Laboratories, Shionogi & Co., Ltd and Dr Ryo Shimizu of Lead Generation Research Laboratory, Tanabe Seiyaku Co., Ltd for the calculation of the atomic charges by CNDO/2 and gaussian 90 (STO-3G), respectively. This study was supported, in part, by Grants-in-Aid for Scientific Research from the Ministry of Education, Science and Culture of Japan.

REFERENCES

1. Ghiasuddin, S. M. & Matsumura, F., Inhibition of gamma-aminobutyric acid (GABA)-induced chloride uptake by gamma-BHC and heptachlor epoxide. *Comp. Biochem. Physiol.*, **73C** (1982) 141–4.
2. Matsumura, F. & Ghiasuddin, S. M., Evidence for similarities between cyclodiene type insecticides and picrotoxinin in their action mechanisms. *J. Environ. Sci. Health*, **B18** (1983) 1–14.
3. Tanaka, K., Scott, J. G. & Matsumura, F., Picrotoxinin receptor in the central nervous system of the American cockroach: Its role in the action of cyclodiene-type insecticides. *Pestic. Biochem. Physiol.*, **22** (1984) 117–27.
4. Lawrence, L. J. & Casida, J. E., Interactions of lindane, toxaphene and cyclodienes with brain-specific *t*-butylbicyclophosphorothionate receptor. *Life Sci.*, **35** (1984) 171–8.
5. Abalis, I. M., Eldefrawi, M. E. & Eldefrawi, A. T., High-affinity stereospecific binding of cyclodiene insecticides and γ-hexachlorocyclohexane to γ-aminobutyric acid receptors of rat brain. *Pestic. Biochem. Physiol.*, **24** (1985) 95–102.
6. Casida, J. E. & Palmer, C. J., 2,6,7-Trioxabicyclo[2.2.2] octanes: Chemistry, toxicology and action at the GABA-gated chloride channel. In *Chloride Channels and Their Modulation by Neurotransmitters and Drugs*, ed. G. Biggio & E. Costa. Raven Press, New York, 1988, pp. 109–23.
7. Ozoe, Y., Sawada, Y., Mochida, K., Nakamura, T. & Matsumura, F., Structure–activity relationships in a new series

of insecticidally active dioxatricycloalkenes derived by structural comparison of the GABA antagonists bicycloorthocarboxylates and endosulfan. *J. Agric. Food Chem.*, **38** (1990) 1264–8.
8. Ozoe, Y., Takayama, T., Sawada, Y., Mochida, K., Nakamura, T. & Matsumura, F., Synthesis and structure–activity relationships of a series of insecticidal dioxatricyclododecenes acting as the noncompetitive antagonists of $GABA_A$ receptors. *J. Agric. Food Chem.*, **41** (1993) 2135–41.
9. Ozoe, Y. & Matsumura, F., Structural requirements for bridged bicyclic compounds acting on picrotoxinin receptor. *J. Agric. Food Chem.*, **34** (1986) 126–34.
10. Cramer, R. D., III, Patterson, D. E. & Bunce, J. D., Comparative molecular field analysis (CoMFA). 1. Effect of shape on binding of steroids to carrier proteins. *J. Am. Chem. Soc.*, **110** (1988) 5959–67.
11. Squires, R. F., Casida, J. E., Richardson, M. & Seaderup, E., [^{35}S]*t*-Butylbicyclophosphorothionate binds with high affinity to brain-specific sites coupled to γ-aminobutyric acid-A and ion recognition sites. *Mol. Pharmacol.*, **23** (1983) 326–36.
12. Fujita, T., Iwasa, J. & Hansch, C., A new substituent constant, π, derived from partition coefficients. *J. Am. Chem. Soc.*, **86** (1964) 5175–80.
13. Callahan, M. A., Slimak, M. W., Gabel, N. W., May, I. P., Fowler, C. F., Freed, J. R., Jennings, P., Durfee, R. L., Whitmore, F. C., Maestri, B., Mabey, W. R., Holt, B. R. & Gould, C., EPA-440/4-79-029a (1979).
14. Hermens, J. & Leeuwangh, P., Joint toxicity of mixtures of 8 and 24 chemicals to the guppy (*Poecilia reticulata*). *Ecotox. Envir. Safety*, **6** (1982) 302–10.
15. Kurihara, N., Uchida, M., Fujita, T. & Nakajima, M., Studies on BHC isomers and related compounds. V. Some physicochemical properties of BHC isomers (1). *Pestic. Biochem. Physiol.*, **2** (1973) 383–90.
16. Medchem Software, BioByte, PO Box 517, Claremont, California 91711, USA.
17. SYBYL Molecular Modeling Software, Tripos Associates, Inc., St Louis, Missouri.
18. Smith, G., Kennard, C. H. L. & Shields, K. G., Insecticides. XI. Crystal structure of endosulfan, β-6,7,8,9,10,10-hexachloro-1,5,5a,6,9,9a-hexahydro-*endo*-6,9-methano-2,4,3-benzodioxathiepin 3-oxide. *Aust. J. Chem.*, **30** (1977) 911–6.
19. Smith, G., Kennard, C. H. L. & White, A. H., Insecticides. Part V. Crystal structures of β-(*eeeeee*)-1,2,3,4,5,6-hexachlorocyclohexane and γ-(*aaaeee*)-1,2,3,4,5,6-hexachlorocyclohexane (lindane) (redeterminations). *J. Chem. Soc. Perkin II*, (1976) 614–5.
20. Mackay, M. F. & Sadek, M., The crystal and molecular structure of picrotoxinin. *Aust. J. Chem.*, **36** (1983) 2111–7.
21. Nimrod, D. M., Fitzwater, D. R. & Verkade, J. G., The crystal structure of the bicyclic phosphate $OP(OCH_2)_3CCH_3$. *J. Am. Chem. Soc.*, **90** (1968) 2780–4.
22. Hata, T., Furukawa, Y., Ozoe, Y. & Matsumura, F., Crystal structure of 5-(3-phenoxyphenyl)-2,3 : 8,7-*endo*-4,6-dioxatricyclo[7.2.1.$0^{2,8}$] dodec-10-ene. *Anal. Sci.*, **7** (1991) 669–70.
23. MOPAC Ver.5, J. J. P. Stewart, Quantum Chemistry Program Exchange, Program no. 455, Indiana University, Bloomington, Indiana.
24. Stewart, J. J. P., Optimization of parameters for semi-empirical methods I. Method. *J. Compt. Chem.*, **10** (1989) 209–20.
25. Stewart, J. J. P., Optimization of parameters for semi-empirical methods II. Applications. *J. Compt. Chem.*, **10** (1989) 221–64.
26. Frisch, M. J. Head-Gordon, M., Trucks, G. W., Foresman, J. B., Raghavachari, K., Schlegel, H. B., Robb, M., Binkley, J. S., Gonzalez, C., Defrees, D. J., Fox, D. J., Whiteside, R. A., Seeger, R., Melius, C. F., Baker, J., Kahn, L. R., Stewart, J. J. P., Fluder, E. M., Topiol, S. & Pople, J. A., Gaussian 90, Gaussian, Inc., Pittburgh, PA, 1990.
27. Dewar, M. J. S. & Thiel, W., Ground states of molecules. 38. The MNDO method. Approximations and parameters. *J. Am. Chem. Soc.*, **99** (1977) 4899–906.
28. Dewar, M. J. S. & Thiel, W., Ground states of molecules. 39. The MNDO method. Approximations and parameters. *J. Am. Chem. Soc.*, **99** (1977) 4907–17.
29. Pople, J. A. & Segal, G. A., Approximate self-consistent molecular orbital theory. III. CNDO results for AB_2 and AB_3 systems. *J. Chem. Phys.*, **44** (1966), 3289–96.
30. Lindberg, W., Persson, J. A. & Wold, S., Partial least-squares method for spectrofluorimetric analysis of mixtures of humic acid and lignin sulfonate. *Anal. Chem.*, **55** (1983) 643–8.
31. Akamatsu, M., Fujita, T., Ozoe, Y., Mochida, K., Nakamura, T. & Matsumura, F., 3D QSAR of insecticidal dioxatricycloalkene and its related compounds. In *Trends in QSAR and Molecular Modelling 92*, ed. C. G. Wermuth. ESCOM Science Publishers B. V., Leiden, 1993, pp. 525–6.
32. Akamatsu, M., Nishimura, K., Osabe, H., Ueno, T. & Fujita, T., Quantitative structure–activity studies of pyrethroids. 29. Comparative molecular field analysis (three-dimensional) of the knockdown activity of substituted benzyl chrysanthemates and tetramethrin and related imido- and lactam-*N*-carbinyl esters. *Pestic. Biochem. Physiol.*, **48** (1994) 15–30.
33. Kiso, M., Fujita, T., Kurihara, N., Uchida, M., Tanaka, K. & Nakajima, M., Structure–activity relationship of lindane analogs. *Pestic. Biochem. Physiol.*, **8** (1978) 33–43.
34. McNamara, B. P. & Krop, S., Observations on the pharmacology of the isomers of hexachlorocyclohexane. *J. Pharmacol. Exp. Ther.*, **92** (1948) 140–6.
35. Woodward, R. M., Polenzani, L. & Miledi, R., Effects of hexachlorocyclohexanes on γ-aminobutyric acid receptors expressed in *Xenopus* oocytes by RNA from mammalian brain and retina. *Mol. Pharmacol.*, **41** (1992) 1107–15.
36. Palmer, C. J. & Casida, J. E., Two types of cage convulsant action at the GABA-gated chloride channel. *Toxicol. Lett.*, **42** (1988) 117–22.
37. Deng, Y., Palmer, C. J. & Casida, J. E., House fly head GABA-gated chloride channel: Four putative insecticide binding sites differentiated by [^{3}H]EBOB and [^{35}S]TBPS. *Pestic. Biochem. Physiol.*, **47** (1993) 98–112.
38. Calder, J. A., Wyatt, J. A., Frenkel, D. A. & Casida, J. E., CoMFA validation of the superposition of six classes of compounds which block GABA receptors non-competitively. *J. Comput.-Aided Mol. Design*, **7** (1993) 45–60.
39. Cole, L. M., Saleh, M. A. & Casida, J. E., House fly head GABA-gated chloride channel: [^{3}H] α-endosulfan binding in relation to polychlorocycloalkane insecticide action. *Pestic. Sci.*, **42** (1994) 59–63.
40. Ffrench-Constant, R. H., The molecular and population genetics of cyclodiene insecticide resistance. *Insect Biochem. Molec. Biol.*, **24** (1994) 335–45.